Copy
RM L9D15

NACA RM L9D15

NACA

RESEARCH MEMORANDUM

HYDRODYNAMIC CHARACTERISTICS OF

A SWEPT PLANING-TAIL HULL

By Robert E. McKann, Claude W. Coffee,
and Donald D. Arabian

Langley Aeronautical Laboratory
Langley Air Force Base, Va.

NATIONAL ADVISORY COMMITTEE
FOR AERONAUTICS

WASHINGTON
September 12, 1949

NATIONAL ADVISORY COMMITTEE FOR AERONAUTICS

RESEARCH MEMORANDUM

HYDRODYNAMIC CHARACTERISTICS OF A SWEPT PLANING-TAIL HULL

By Robert E. McKann, Claude W. Coffee, and Donald D. Arabian

SUMMARY

The hydrodynamic characteristics of a swept planing-tail hull were determined by tests in Langley tank no. 2. The hull was derived from an aerodynamically refined planing-tail hull by sweeping aft the water planes above the chines. This procedure resulted in an aft movement of the hull volume which produced a more favorable volume distribution about the center of gravity. With vertical spray strips, only light spray struck the propellers over a short speed range before the hump. No spray came over the bow. Heavy spray struck the tail surfaces near hump speed. A large range of elevator deflection was available for take-offs over a wide range of center-of-gravity location. The minimum trim of 2° at high speed rather than lower-limit porpoising determined the minimum elevator deflection for take-off. Upper-limit porpoising occurred over a short speed range near take-off. Landings at locations of the center of gravity from $0.20\bar{c}$ to $0.40\bar{c}$ were stable. The hump load-resistance ratio of 3.1 was lower than ratios obtained for conventional hulls.

INTRODUCTION

Several refinements of the planing-tail-type flying-boat hull have been made to decrease its drag. The refinements include the use of symmetrical airfoil sections for the forebody plan form and slender boom-like afterbodies. Tests of the hulls in the Langley 300 MPH 7- by 10-foot tunnel (see reference 1) indicated drag approaching that of the fuselage of a modern transport airplane. Tank investigations, described in reference 2, showed that the hulls had acceptable hydrodynamic performance.

The problem of airplane balance may limit the application of the hulls to special-purpose, high-performance airplanes, because of the large portion of the total volume forward of the center of gravity. Since the center-of-gravity position was fixed by aerodynamic and hydrodynamic requirements, a possible solution to the balance problem was to move the volume aft. A new hull, the volume of which was shifted aft with respect to the center of gravity by sweeping aft the water planes above the chines, was derived. Wind-tunnel tests of the new hull on a swept wing at low speeds (see reference 3) and high subsonic speeds (see reference 4) were made in the Langley 300 MPH 7- by 10-foot tunnel. These tests indicated drag similar to that of the unswept hull.

A model representative of a full-scale flying boat embodying the swept hull, was tested in Langley tank no. 2. The gross weight of the assumed flying boat was 65,000 pounds but its volume was 60 percent less than that of the Boeing XPBB-1, a conventional flying boat of the same gross weight. The results of the tank tests of the swept hull are given in this paper.

SYMBOLS

C_{Δ_o}	gross load coefficient $\left(\Delta_o/wb^3\right)$
C_{Δ}	load coefficient $\left(\Delta/wb^3\right)$
C_V	speed coefficient $(V/\sqrt{gb})$
C_R	resistance coefficient (R/wb^3)
Δ/R	load-resistance ratio
Δ	load on water, pounds
Δ_o	gross load, pounds
R	resistance, pounds
V	speed, feet per second
g	acceleration of gravity, feet per second per second
b	maximum beam of hull (6.43 ft, full-size)
w	specific weight of water (63.0 lb/cu ft in these tests)
$\bar{c}$	mean aerodynamic chord
τ	trim measured between forebody keel and horizontal, degrees
δ_e	elevator deflection, degrees

MODEL AND APPARATUS

A powered dynamic model of the swept-hull configuration, designated Langley tank model 237-6SB, was used for the tank tests. Photographs of the model are shown in figure 1. The general arrangement and hull lines are presented in figures 2 and 3, respectively. The offsets of the hull are given in table I.

The basic plan-form section of the forebody (modified 16 series symmetrical airfoil section with a thickness ratio of 14.3 percent) was the same as that used for the unswept forebodies of the models in reference 2. However, the water planes above the chine were progressively shifted aft, producing a swept profile as shown in figure 3. The length of the bow was decreased, but the volume was kept about the same by this manner of sweeping the hull. The afterbody was a simple conical boom.

The forebody chine was made straight in profile resulting in a continuous variation in deadrise angle and slightly convex buttock lines near the step. Vertical spray strips were installed at the chine to reduce propeller spray. Spray tests were first made with the spray strip shown in figure 4(a) which has the same depth as that used in reference 2 on the unswept model. Since this spray strip allowed heavy spray to reach the propellers, the one shown in figure 4(b) was developed and used throughout the rest of the tests.

The configuration was a $\frac{1}{16}$-scale model representing an assumed flying boat of 65,000 pounds gross load $\left(C_{\Delta_0} = 3.87\right)$. The wing loading and power loading of the Navy XPBB-1 flying boat (35.6 lb/sq ft and 14.8 lb/bhp) were simulated on the model. The size and locations of the aerodynamic surfaces corresponded to those of the XPBB-1. No flaps were used. The lateral spacing of the nacelles was the same as that of the twin-boom configuration described in reference 2. Leading-edge slats were installed to compensate for the low Reynolds number of the tests. The elevators had a range of deflection from -30° to 20°.

The test setup is shown in figure 5 with the model under way at a speed coefficient of 8.3. The model was free to trim about the pivot, which was located at the center of gravity and was free to move vertically, but was restrained in roll and yaw.

PROCEDURE

Spray

The range of speed over which spray was in the propellers was determined by making constant speed runs at full power and a series of gross loads. The model was free to trim about the 0.30$\bar{c}$ location of the center of gravity with the elevators fixed at 0°. Observations were made of bow spray and spray that struck the wing and tail surfaces.

Take-off Stability

In order to find the trim limits of stability, the towing carriage was held at constant speeds, while the model trim was slowly increased or decreased until the porpoising limit was crossed. The variation of trim with speed for three locations of the center of gravity ($0.20\bar{c}$, $0.30\bar{c}$, and $0.40\bar{c}$) was determined during accelerated runs (1.0 ft/sec^2) to take-off with full power and fixed elevators. The range of available center-of-gravity and elevator positions that would permit operation at trims above 2° without porpoising of greater than 2° amplitude was investigated during accelerated runs. A minimum trim of 2° appeared to be a reasonable limit for purposes of evaluation.

Landing Stability

The landing stability was investigated by trimming the model in the air to the desired landing trim, while the carriage was held at a constant speed slightly above the model flying speed, and then decelerating the carriage at a constant rate of 3 feet per second per second, allowing the model to glide onto the water in simulation of an actual landing. The descent to the water from flight was made from a height of 0.3b above the water. This method was used to hold the sinking speeds to a value of approximately 300 feet per minute. After the first contact the rise restriction was removed. Landings were made with the center of gravity located at $0.20\bar{c}$, $0.30\bar{c}$, and $0.40\bar{c}$, using one-quarter thrust.

Resistance

The resistance characteristics were obtained with the wing and tail surfaces removed. Constant speed runs were made with the model fixed in trim. Lift curves (assuming lift to vary as the square of the speed) were calculated for the model from the take-off speeds observed for various trims during the take-off stability tests. The load on the water, applied by dead weights, was determined from the lift curves. The range of trim tested at each speed was the range of stable trim obtained at that speed during the stability tests with the center of gravity located at $0.30\bar{c}$ except in the speed range from $C_V = 6.0$ to take-off where the maximum trim was arbitrarily limited to 12°. The resistance selected was the lowest resistance obtained at each speed.

RESULTS AND DISCUSSION

Spray Characteristics

The gross load coefficient at which spray entered the propellers with the two spray-strip arrangements shown in figure 4 is plotted against speed coefficient in figure 6. With the spray strip of the same depth as that used on the unswept models of reference 2, the propeller spray was too heavy to be considered acceptable. This heavy spray resulted from the shorter forebody, shorter spray strip, and the lower trim which allowed spray to flow around the forward end of the spray strip. This undeflected spray was heavier than the light intermittent spray coming from under the strips. Lengthening and deepening the spray strip to give the arrangement shown in figure 4(b) not only reduced the intensity of spray in the propellers at the design gross load but also decreased the ranges of speed and load coefficients over which spray struck the propellers. The propeller spray was considered to be light at the design gross load with the final configuration used. The worst spray condition for the two spray-strip arrangements is shown in figure 7.

In practice, the spray strips could be retracted in sections. However, unpublished wind-tunnel tests on the unswept model of reference 2 indicate that the drag of such spray strips may not be enough to warrant retraction.

In spite of the low bow clearance there was no spray over the bow during take-off runs. The tail surfaces were struck by heavy spray from the forebody roach near hump speed over a speed-coefficient range of about 0.3. At high speeds only light spray from the forebody wetted the tail surfaces and the under surface of the inboard wing panels.

Take-Off Stability and Trims

The trim limits of stability of the swept-hull model are compared with those of the unswept model in figure 8. The differences between the two lower-limit curves are not large, the peak for the swept hull being 10.5°. Upper-limit porpoising was obtained for the swept hull during constant speed runs over a short speed range ($C_V = 6.3$ to 7.7) near take-off.

In figure 9, trim is plotted against speed coefficient for various elevator deflections at three locations of the center of gravity. The static trim (approximately 7°) was less than that of the unswept model (approximately 10°) as a result of the rearward shift of volume. A trim peak of about 12° was reached near a speed coefficient of 3.5. This peak corresponded to that obtained with the twin-boom configuration. (See reference 2.) The second trim peak that occurred in most of the curves was caused by the action of the roach on the tail boom. Some indication of this peak was found with the single-boom configuration of reference 2. At the aft location of the center of gravity, with large up-elevator deflections, trim increased from rest until the model was near take-off. Aerodynamic tests with the model free to trim indicated that the effectiveness of the elevators in trimming the model began to decrease with an increase in elevator deflections greater than -15°. A wide range of trim was obtainable beyond the hump speed for all center-of-gravity locations.

Typical photographs of the model during these take-off runs are presented in figure 10. The deep draft and small bow clearance at low speeds are shown in figure 10(a). The high trims beyond hump speed, shown in figure 10(a), enables the low bow to be well clear of the water, but keeps the tail boom in the forebody spray. At high speeds and low trims, figure 10(c) shows that only the point of the step is in the water and the bow has ample clearance.

The range of elevator deflection available for take-offs is plotted against location of the center of gravity in figure 11. A large range of elevator deflection was available at all center-of-gravity locations. Neither lower-limit nor upper-limit porpoising determined these elevator limits. Maximum up-elevator deflection resulted in no upper-limit porpoising greater than 2° amplitude. It is apparent from figure 9 that 2° minimum trim at high speed will be reached before 2° amplitude of lower-limit porpoising. The minimum elevator deflection for take-off was therefore determined by the minimum trim of 2° rather than by the lower-limit porpoising.

Landing Stability

The amplitudes of the maximum oscillations of trim during landing are plotted against contact trims in figure 12(a). In figure 12(b) the amplitudes of the maximum vertical motions, at the center of gravity, are plotted against contact trims. From these plots it is seen that there was little change in rise or trim during any landing and all landings were considered stable. The model trimmed down at contact, since the center of gravity was located well forward of the step point. This contact rotation is plotted against contact trim in figure 13 for the center-of-gravity locations tested.

Resistance

In figure 14, resistance coefficient, load-resistance ratio, load coefficient, and trim are plotted against speed coefficient. The hump load-resistance ratio of 3.1 at a speed coefficient of 3.25 is lower than that obtained with well-designed conventional hulls. The power in the model would not be sufficient for take-off, but in a high-performance airplane considerably more thrust would be available.

Directional Stability

The model was attached to a tubular staff which was slightly flexible torsionally and a tendency to yaw was noticed over a range of speed coefficient from 2.9 to 4.2. Apparently the roach, which impinged on the boom throughout this range, caused the same instability as found in reference 2 on an unswept single-boom hull. The results of unpublished tests with the model in a free, self-propelled condition indicate that the model can be directionally controlled without the use of asymmetric power.

CONCLUSIONS

The results of tests to determine the hydrodynamic characteristics of the swept planing-tail flying-boat lead to the following conclusions:

1. With vertical spray strips, only light spray struck the propellers over a short speed range before the hump. No spray came over the bow. Heavy spray from the forebody roach struck the tail surfaces over a short speed range near the hump speed. Light spray wetted the under surface of the wing at high speeds.

2. Although the peak of the lower limit was high (10.5°), a minimum trim of 2° at high speed rather than lower-limit porpoising determined the minimum elevator deflection for take-off.

3. Upper-limit porpoising occurred over a short speed range near take-off.

4. A large range of elevator deflection was available for take-offs over a wide range of center-of-gravity locations.

5. All landings at center-of-gravity locations from $0.20\bar{c}$ to $0.40\bar{c}$ were stable.

6. The hump load-resistance ratio of 3.1 was lower than ratios obtained with conventional hulls.

Langley Aeronautical Laboratory
National Advisory Committee for Aeronautics
Langley Air Force Base, Va.

REFERENCES

1. Riebe, John M., and Naeseth, Rodger L.: Aerodynamic Characteristics of a Refined Deep-Step Planing-Tail Flying-Boat Hull with Various Forebody and Afterbody Shapes. NACA RM No. L8F01, 1944.

2. McKann, Robert, and Coffee, Claude W.: Hydrodynamic Characteristics of Aerodynamically Refined Planing-Tail Hulls. NACA RM No. L9B04, 1949.

3. Naeseth, Rodger L., and MacLeod, Richard G.: Aerodynamic Characteristics of an Airfoil-Forebody Swept Flying-Boat Hull with a Wing and Tail Swept Back 51.3° at the Leading Edge. NACA RM No. L9F08, 1949.

4. Riebe, John M., and MacLeod, Richard G.: Preliminary Wind-Tunnel Investigation at High-Subsonic Speeds of Planing-Tail, Blended, and Airfoil-Forebody Swept Hulls. NACA RM No. L9D01, 1949.

[redacted]

TABLE I

OFFSETS OF LANGLEY TANK MODEL 237-6SB

[All dimensions are in inches]

Offsets model scale 1/16																							
Station	Distance to F.P.	Keel above base line	Chine above base line	Half breadth of chine	Height of hull at center line	Radius of boom	Line of centers above base line	1-inch buttock		2-inch buttock		1-inch water line	2-inch water line	3-inch water line	4-inch water line	5-inch water line	6-inch water line	7-inch water line	8-inch water line	9-inch water line	10-inch water line	11-inch water line	12-inch water line
								Upper	Lower	Upper	Lower												
F.P.	0	2.80	2.80	0	2.80																		
1	1.66	1.80	2.64	1.08	3.76			2.80	2.56				0.26	0.92									
2	4.31	.76	2.38	1.64	5.28			4.34	1.72				1.64	1.51	1.15	0.58							
3	6.96	.20	2.11	2.01	6.84			5.86	1.17	2.37	2.05		1.89	1.88	1.64	1.36	0.96						
4	9.62	0	1.84	2.24	8.35			7.44	.82	3.91	1.67		2.24	2.16	1.99	1.79	1.52	1.20	0.65				
5	12.27	0	1.60	2.36	9.72			8.78	.64	5.48	1.36		2.35	2.30	2.20	2.08	1.88	1.66	1.36	.86			
6	14.95	0	1.34	2.41	10.80			9.92	.56	7.00	1.15		2.40	2.39	2.33	2.26	2.14	2.00	1.78	1.46	.91		
7	17.18	0	1.14	2.34	11.52			10.72	.49	8.62	1.00		2.37	2.41	2.39	2.34	2.26	2.20	2.06	1.82	1.44	.80	
8	20.25	0	.82	2.12	12.18			11.53	.40	9.58	.76	2.15	2.28	2.36	2.41	2.40	2.36	2.32	2.24	2.10	1.83	1.36	.48
9	22.91	0	.58	1.73	12.56			12.04	.24	10.32	1.73	1.85	2.04	2.20	2.28	2.36	2.40	2.40	2.36	2.31	2.08	1.70	1.04
10	25.55	0	.28	1.04	12.78			12.42	.26	10.98	3.23	1.33	1.68	1.94	2.12	2.24	2.32	2.36	2.40	2.37	2.24	1.98	1.47
11	28.94	0	0	0	12.85			12.60	2.08	11.58	5.18	.47	.93	1.36	1.70	1.96	2.12	2.24	2.34	2.40	2.36	2.18	1.70
12	30.88	1.10			12.80			12.62	3.27	11.72	6.28		.44	.88	1.30	1.68	1.96	2.14	2.24	2.32	2.38	2.29	1.75
13	33.53	2.62			12.66			12.46	4.78	11.58	7.79			.16	.64	1.08	1.48	1.80	2.04	2.20	2.28	2.20	1.64
14	36.18	4.15			12.52	2.21	10.31		6.28	11.25	9.30					.38	.86	1.30	1.66	1.92	2.18		
15	38.84	5.68			12.39	2.08	10.31		7.82								.14	.60	1.06	1.60	2.06		
16	41.50	7.24			12.24	1.94	10.31												.31	1.40	1.92		
17	44.15					1.80	10.31																
18	46.81					1.64	10.31																
19	49.47					1.50	10.31																
20	52.13					1.37	10.31																
21	54.78					1.22	10.31																
22	57.44					1.08	10.31																
23	60.09					.94	10.31																
24	62.75					.80	10.31																
A.P.	64.34					.71	10.31																

[redacted]

NACA

[redacted]

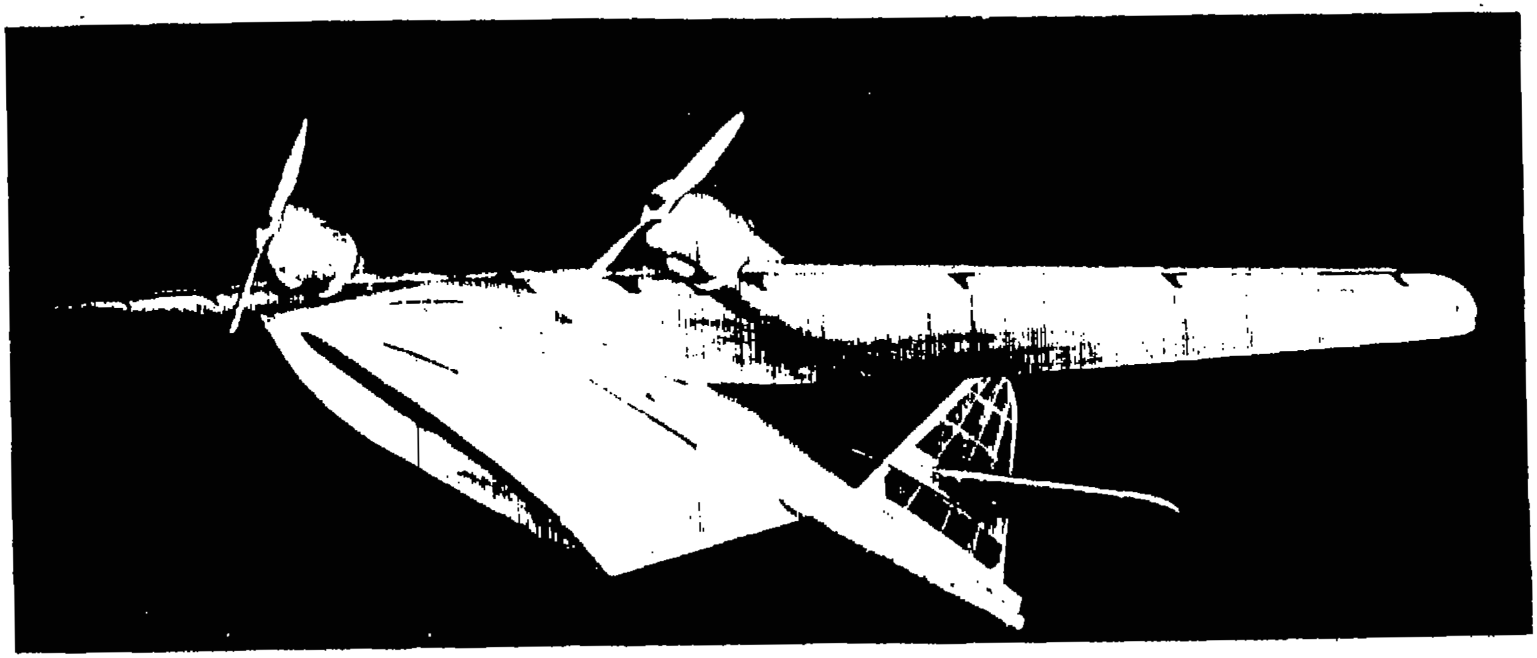

(a) Front view.

NACA

L-56642.1

Figure 1.– Photographs of Langley tank model 237-6SB.

[redacted]

[redacted]

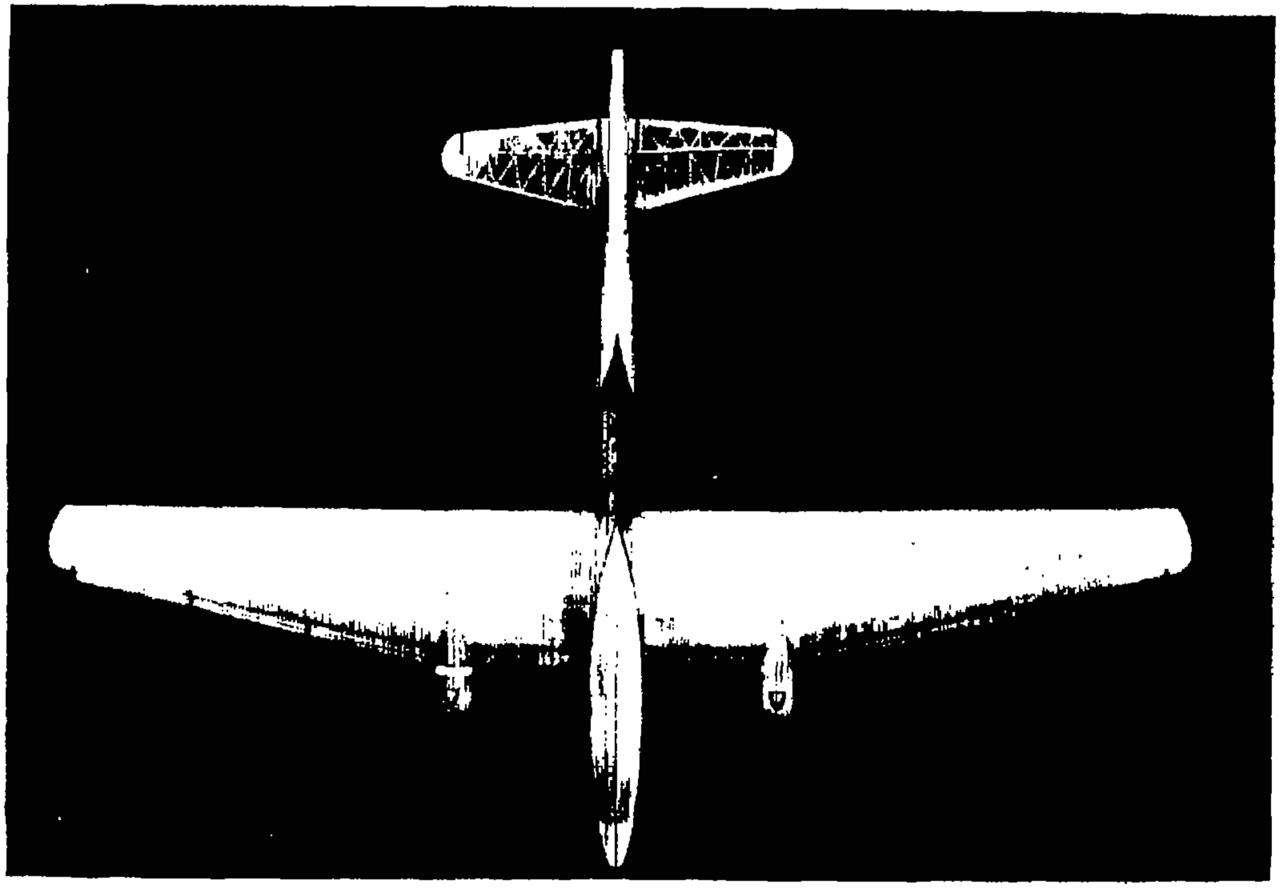

(b) Bottom view.

L-56645.1

Figure 1.– Concluded.

[redacted]

[redacted]

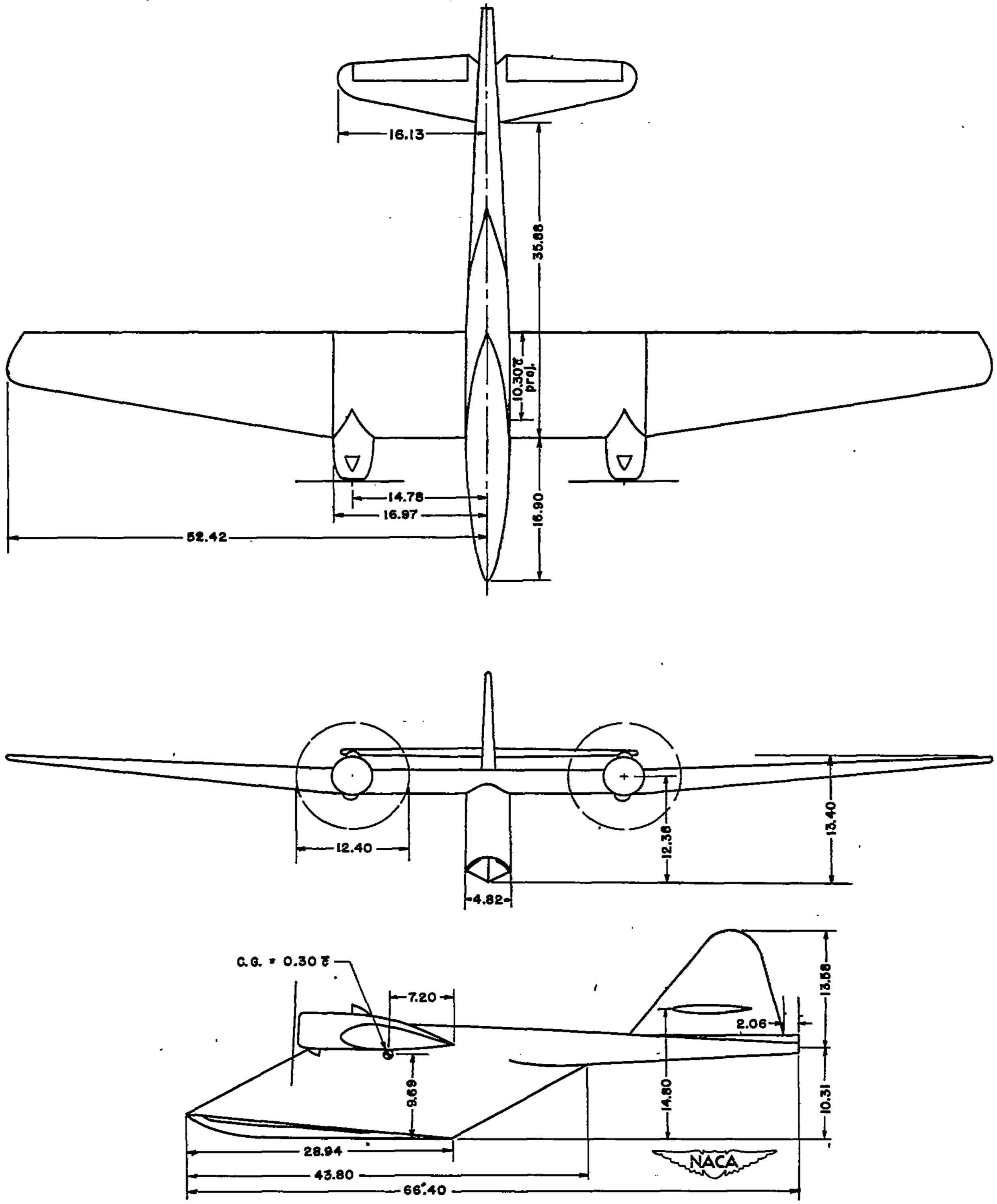

Figure 2.– General arrangement of Langley tank model 237-6SB. (All dimensions in inches.)

[redacted]

[redacted]

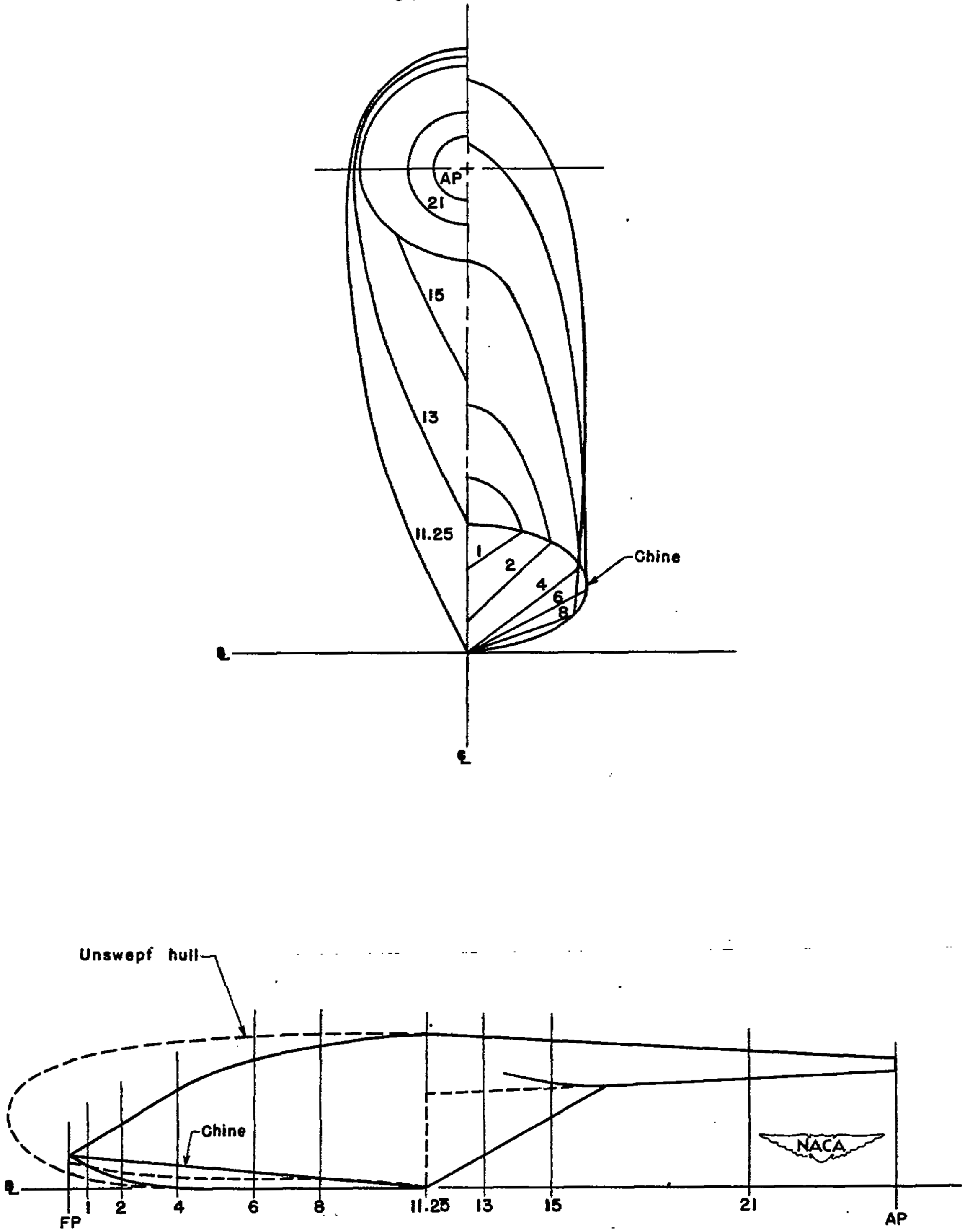

Figure 3.– Hull lines of Langley tank model 237–6SB.

[redacted]

[redacted]

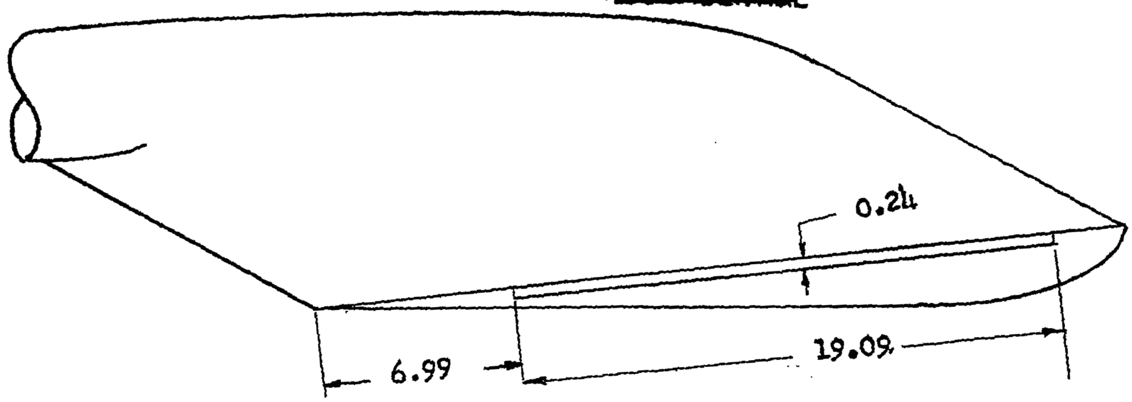

(a) Spray strip similar to that on unswept model.

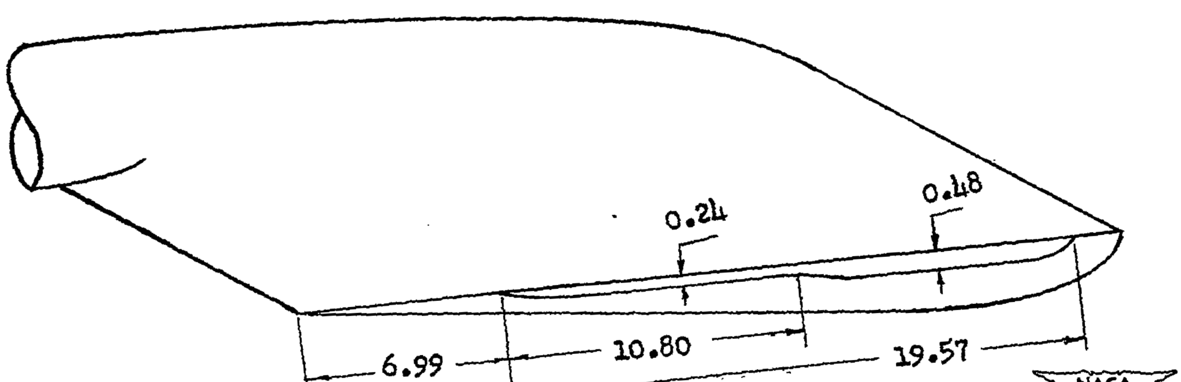

[redacted]

(b) Final spray strip used throughout investigation.

Figure 4.- Spray-strip arrangements. (All dimensions are in inches.)

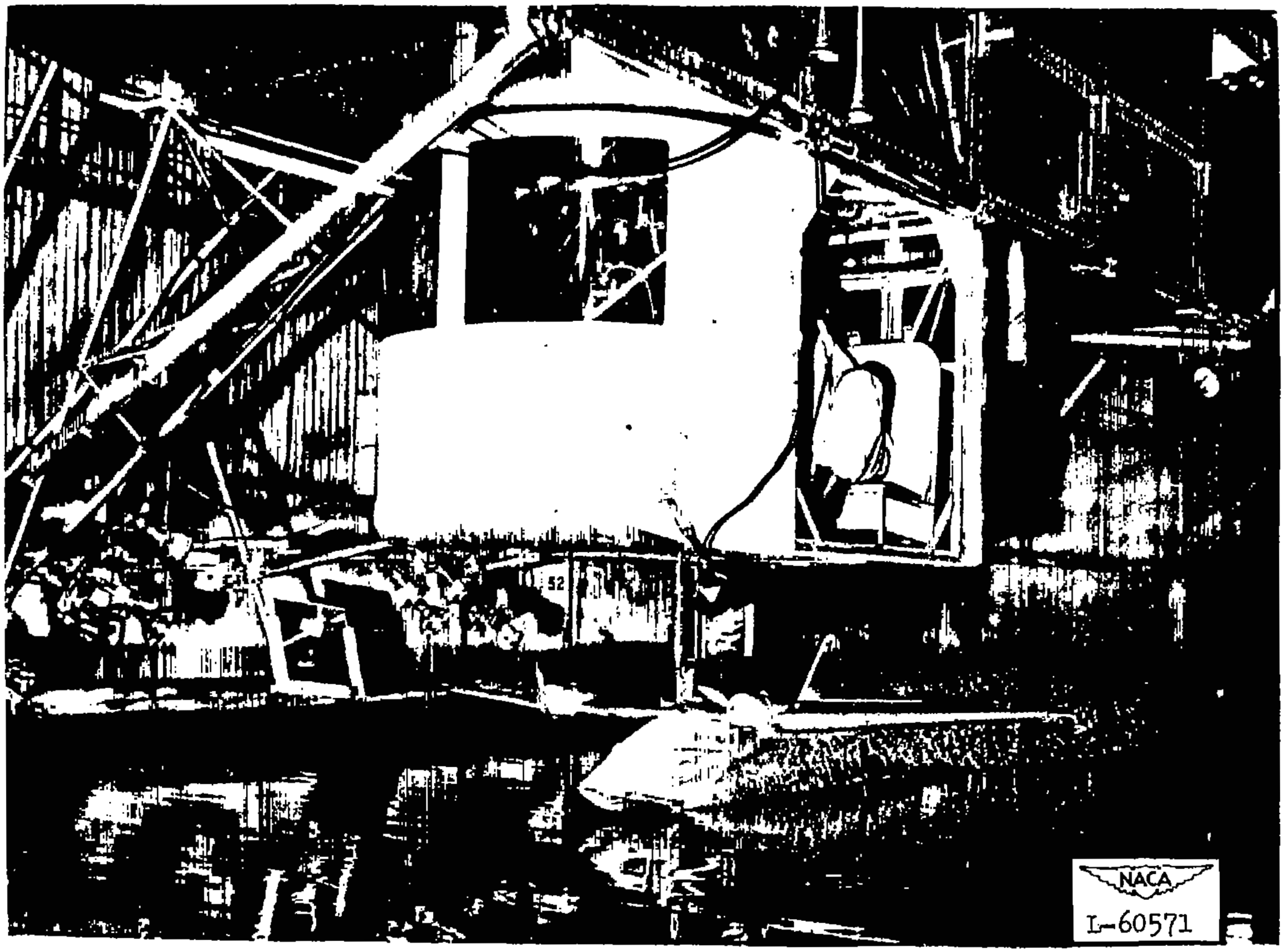

Figure 5.– Test setup.

[redacted]

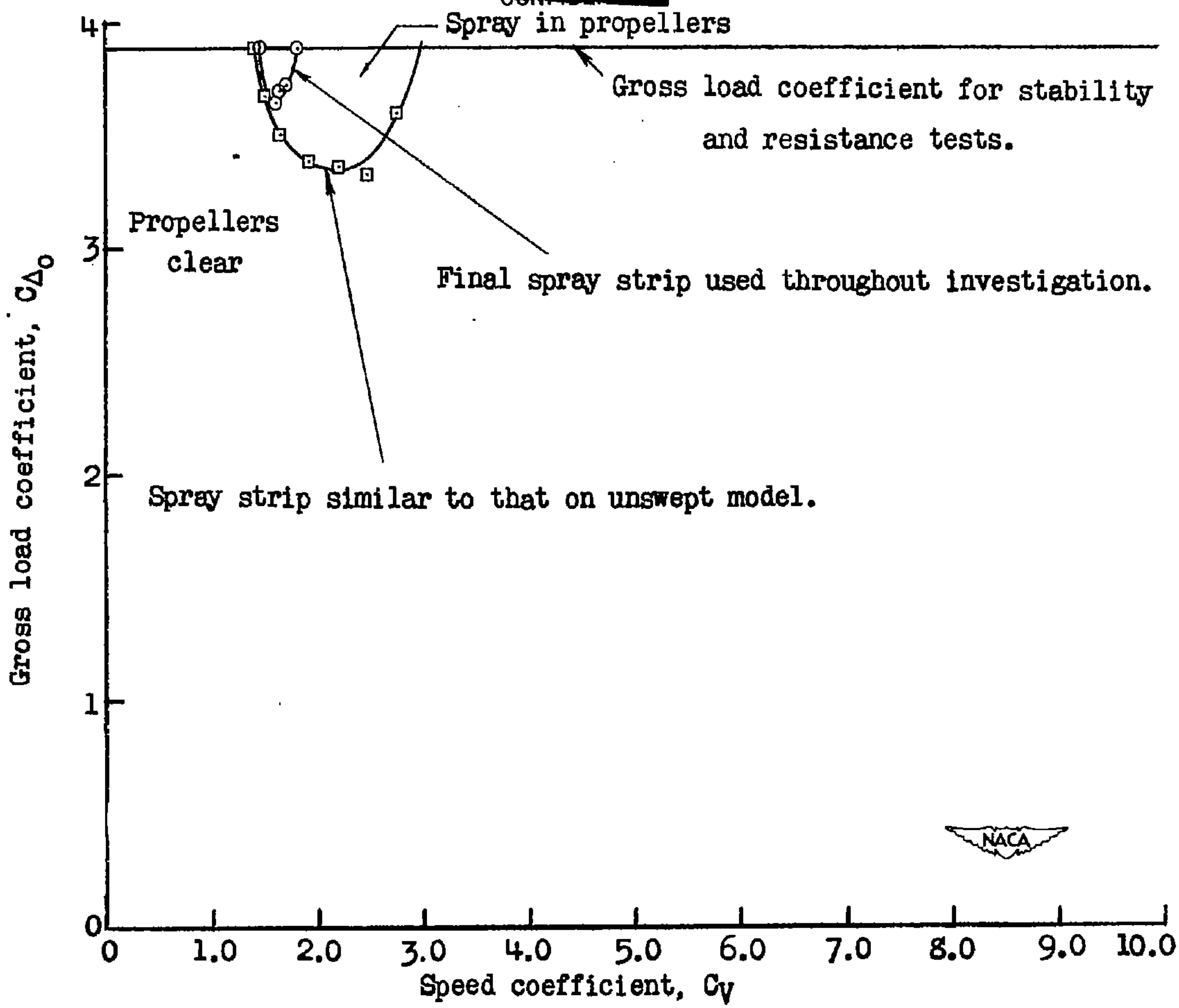

Figure 6.– Gross load coefficients at which spray entered propellers for two spray-strip arrangements.

[redacted]

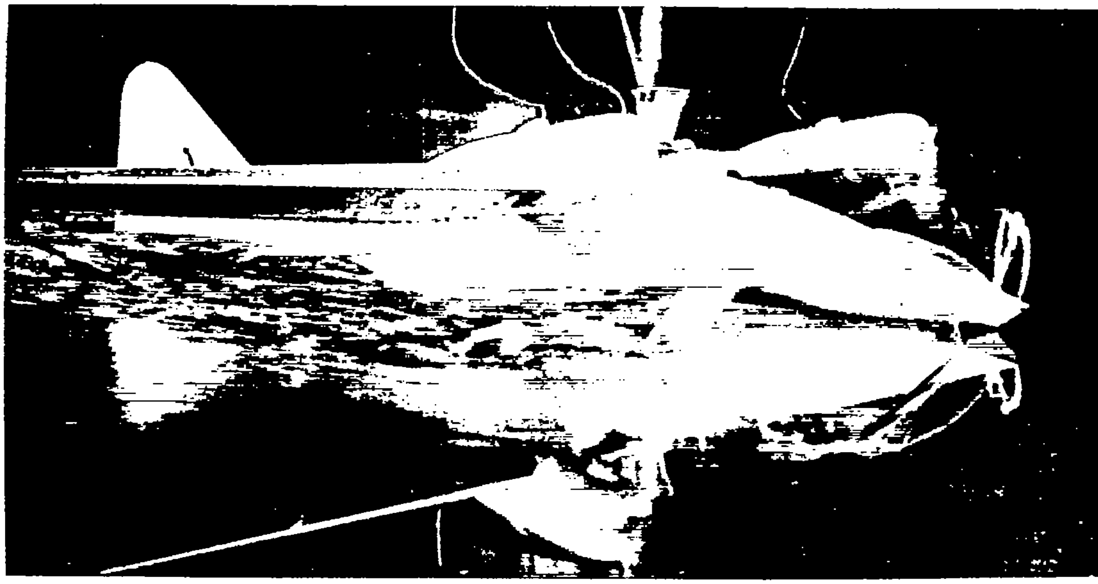

(a) Spray strip similar to that on unswept model.

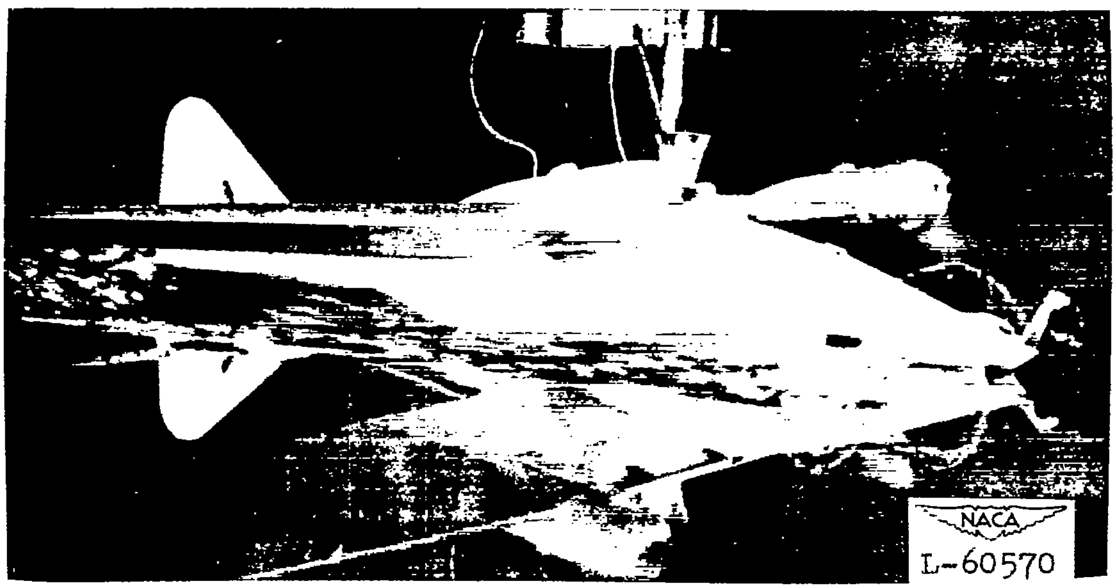

(b) Final spray strip used throughout investigation.

Figure 7.– Worst propeller spray condition for two spray-strip arrangements.

[redacted]

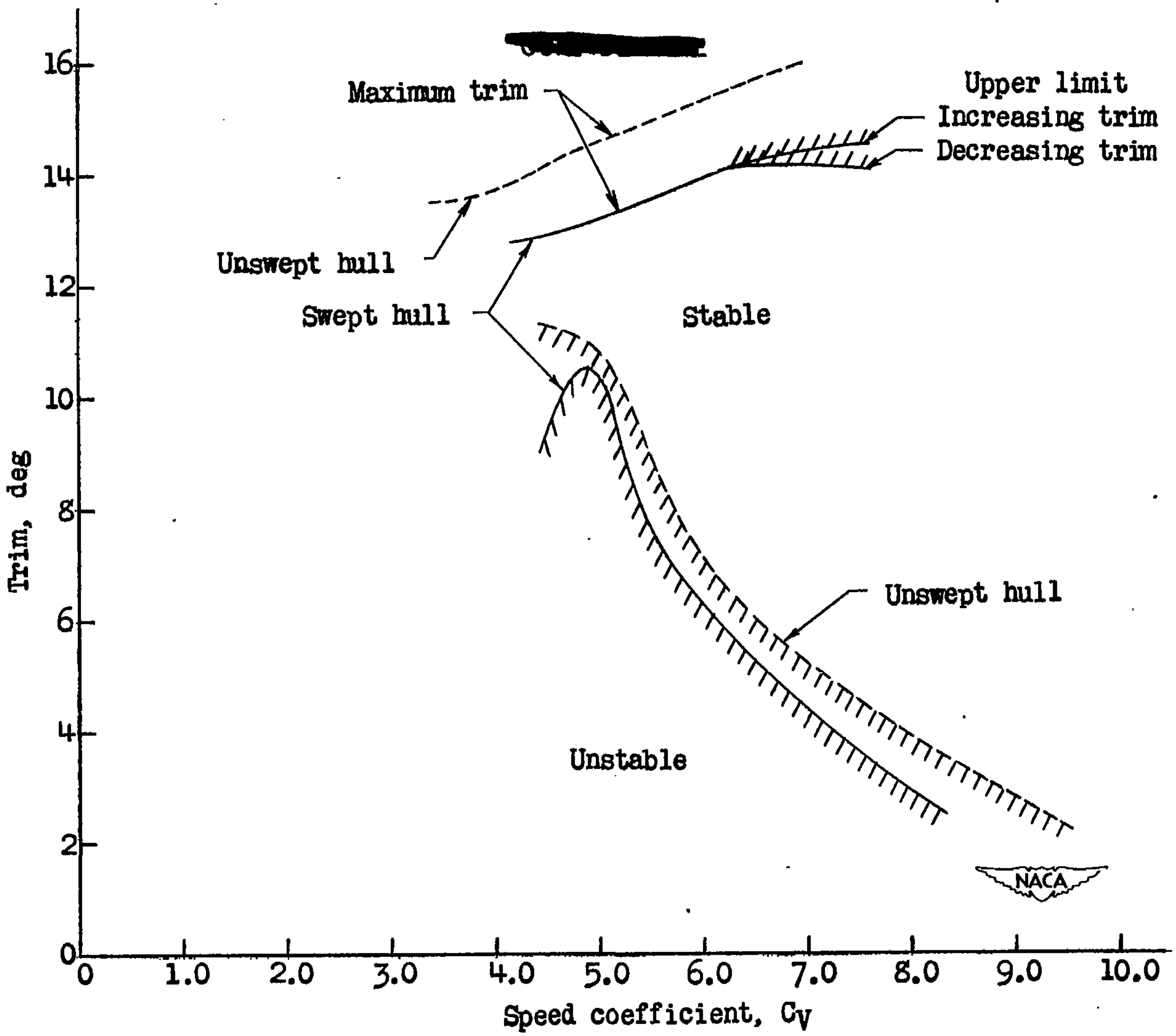

Figure 8.— Trim limits of stability.

[redacted]

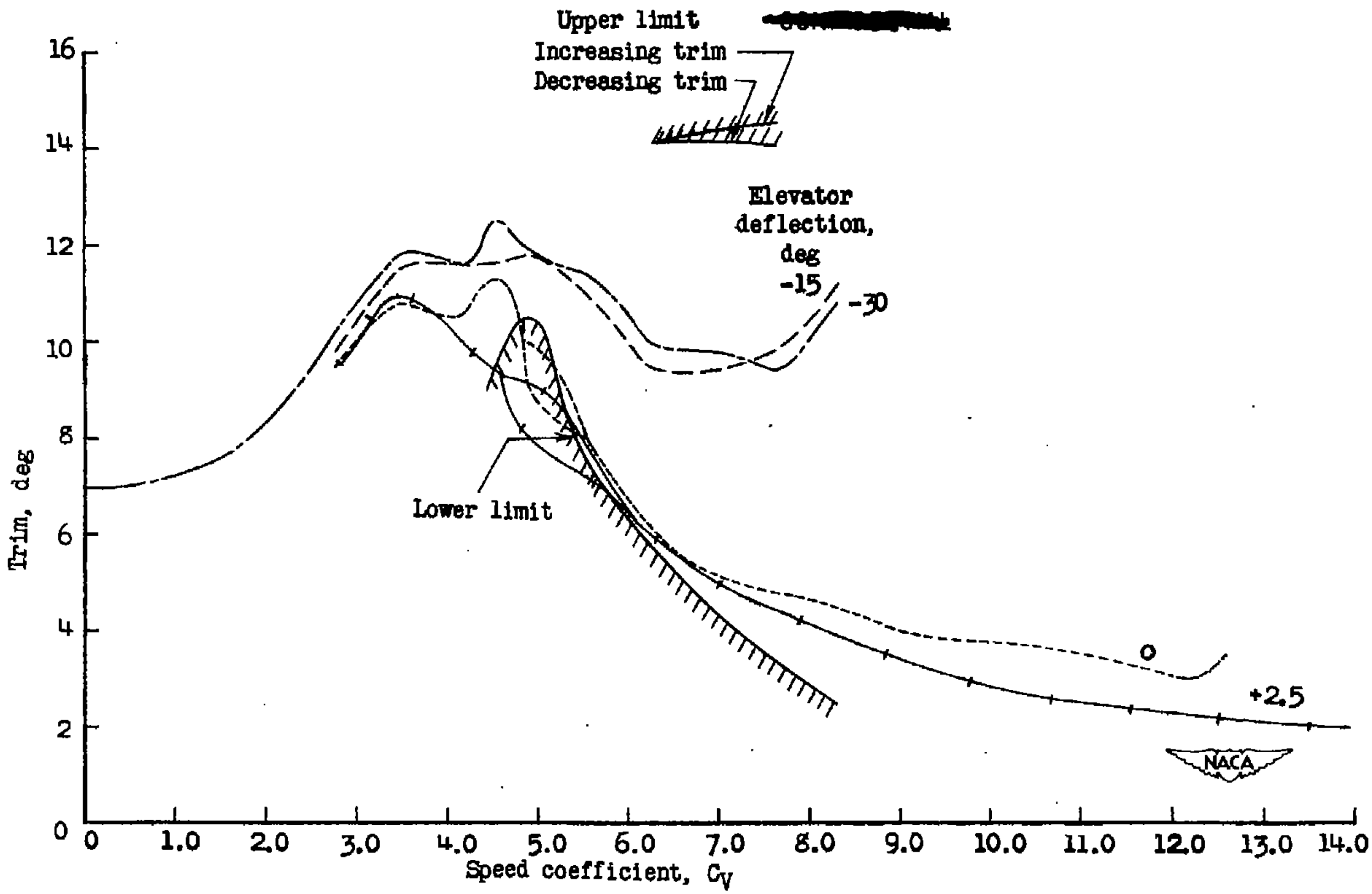

(a) Center of gravity, 0.20 $\bar{c}$.

Figure 9.– Variation of trim with speed coefficient.

[redacted]

[redacted]

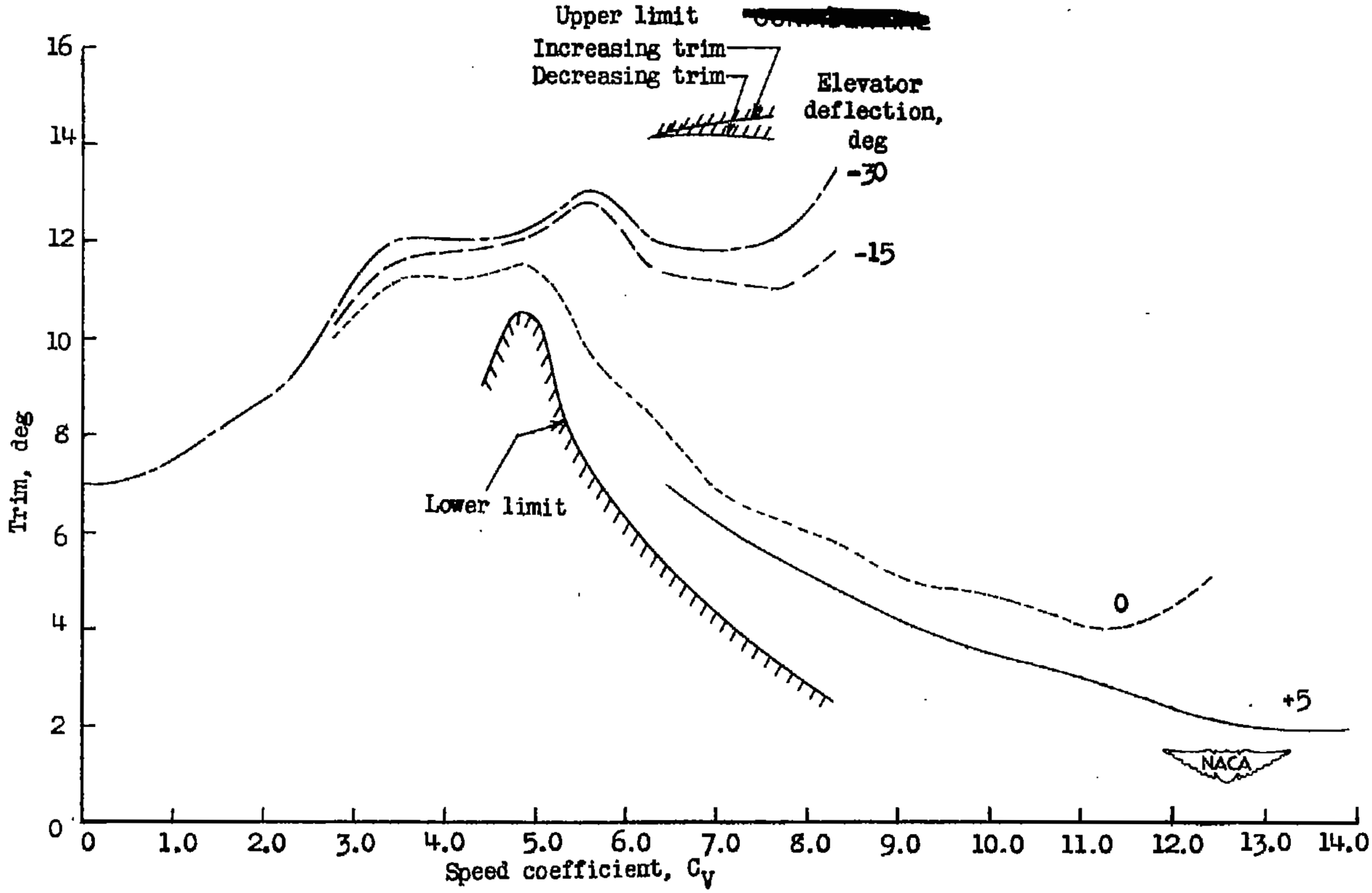

(b) Center of gravity, 0.30 $\bar{c}$.

Figure 9.— Continued.

[redacted]

[redacted]

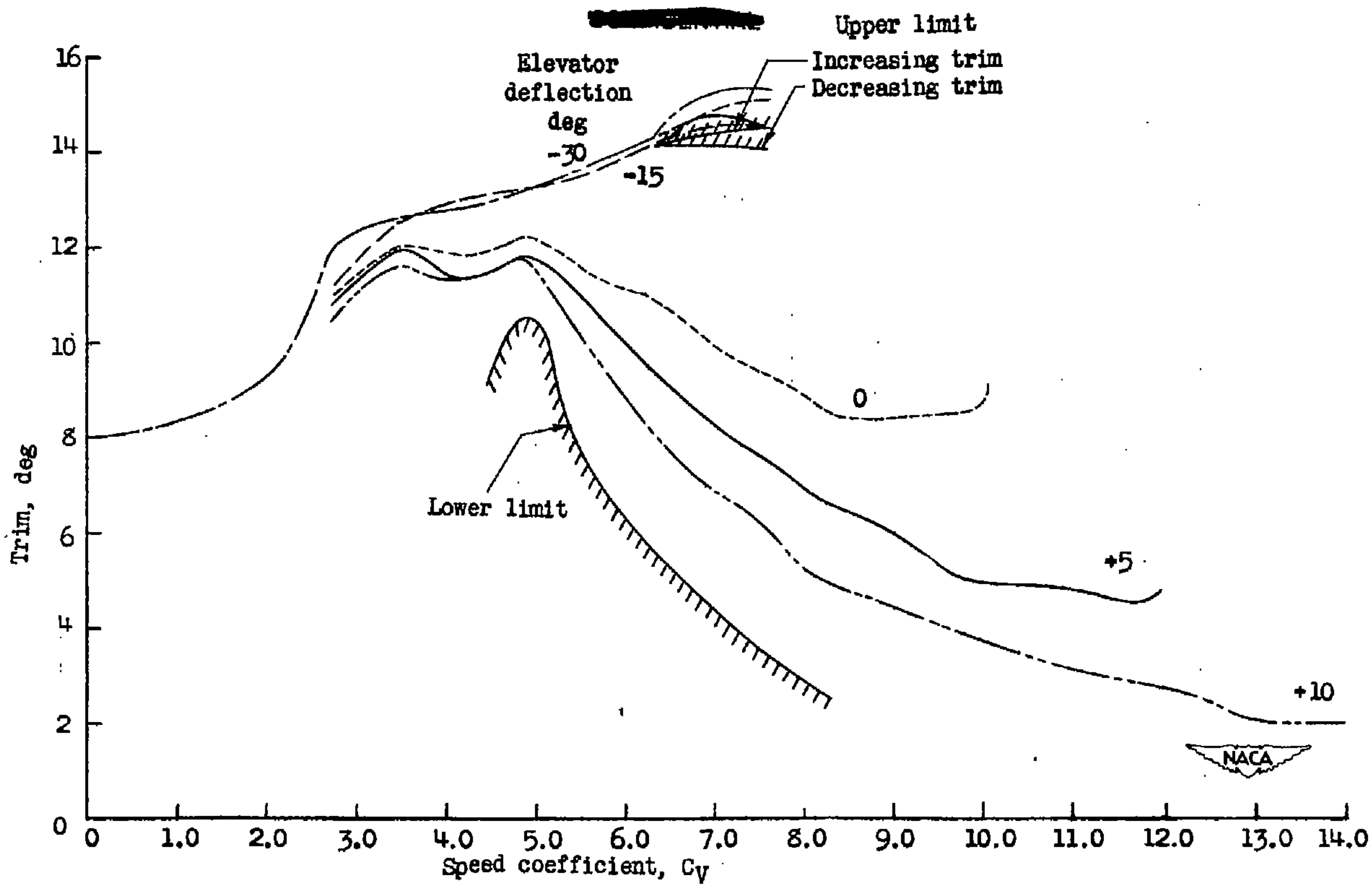

(c) Center of gravity, 0.40 $\bar{c}$.

Figure 9.– Concluded.

[redacted]

(a) $C_V = 2.77$; $\tau = 9.8^\circ$; $\delta_e = -15^\circ$.

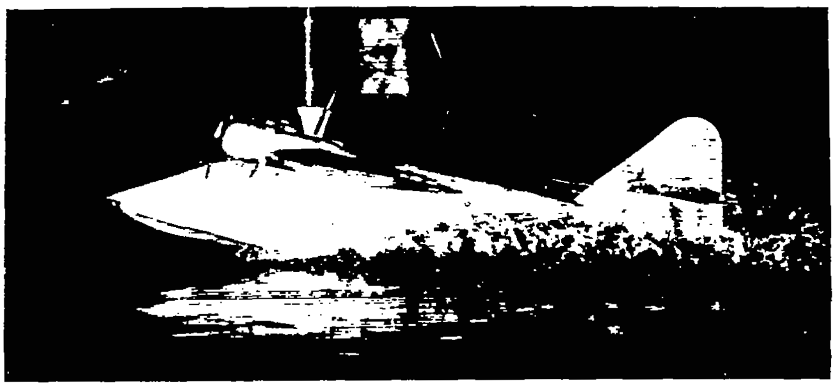

(b) $C_V = 5.54$; $\tau = 11^\circ$; $\delta_e = -10^\circ$.

(c) $C_V = 11.08$; $\tau = 3.5^\circ$; $\delta_e = 0^\circ$.

Figure 10.– Strobo-flash pictures of swept hull being tested. Full power; gross load coefficient, 3.87; center-of-gravity location, 0.20$\bar{c}$. [redacted]

[redacted]

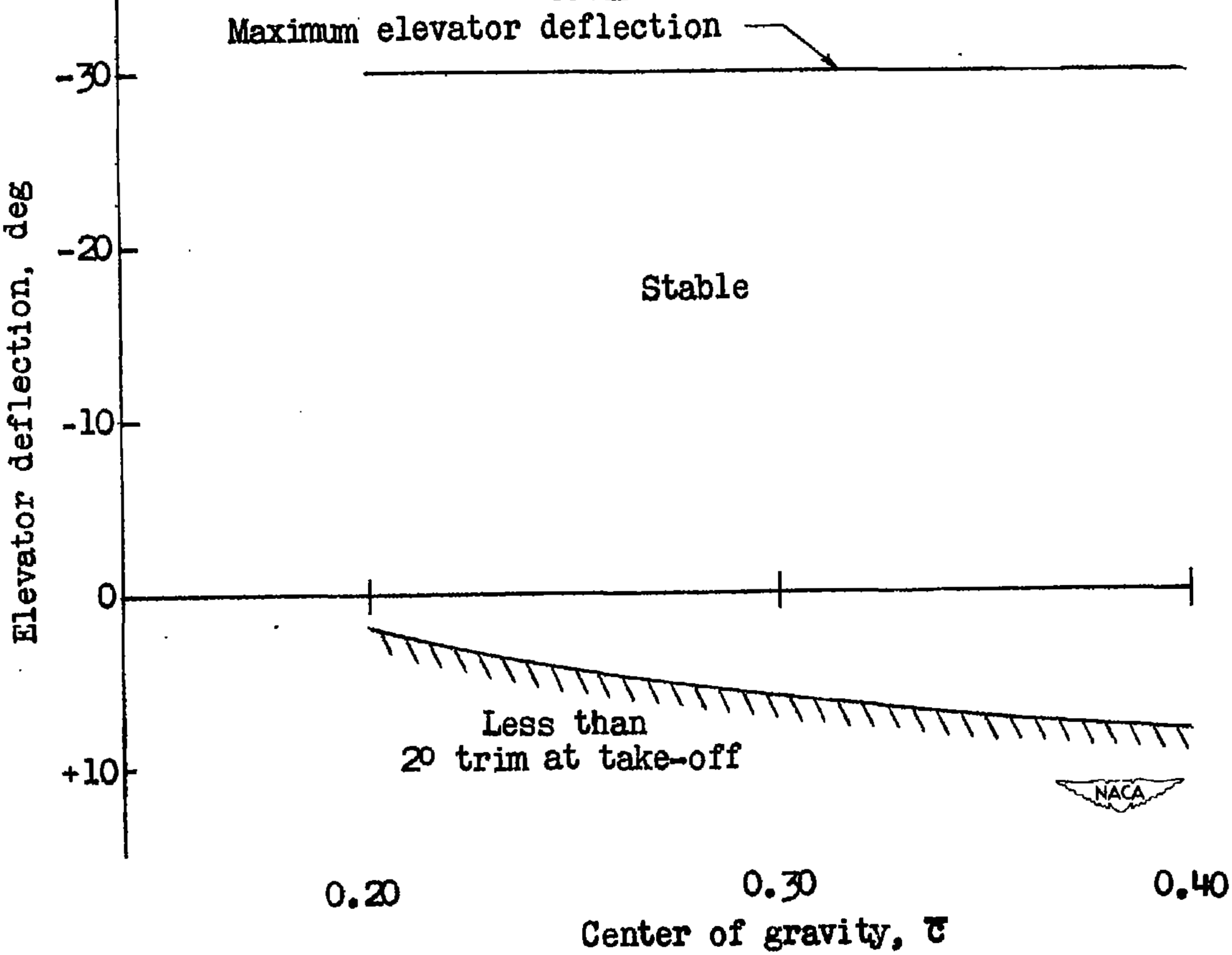

Figure 11.– Elevator limits for various center-of-gravity locations. Gross load coefficient, 3.87, full power.

[redacted]

[redacted]

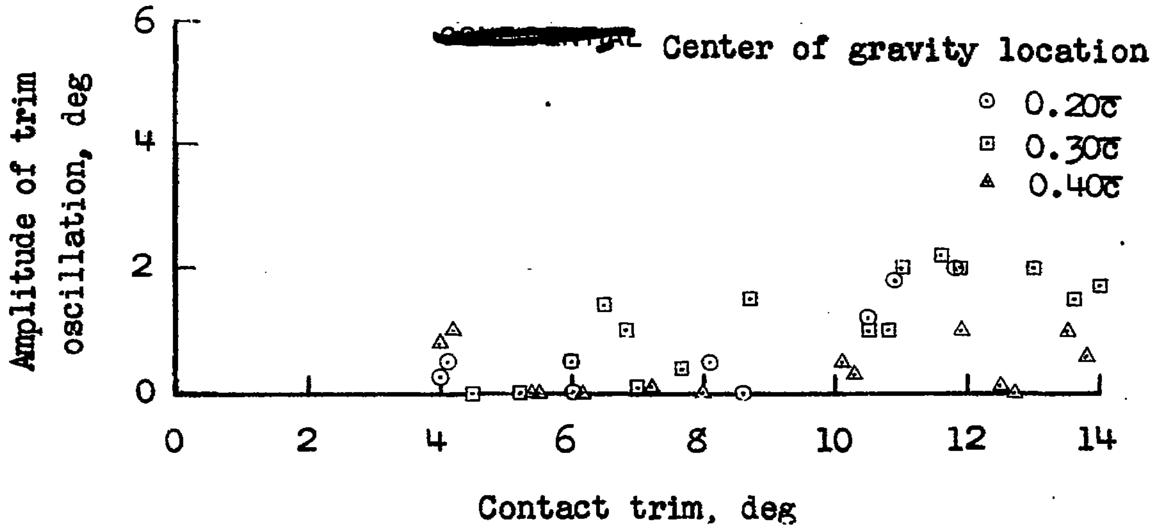

(a) Amplitude of trim oscillations.

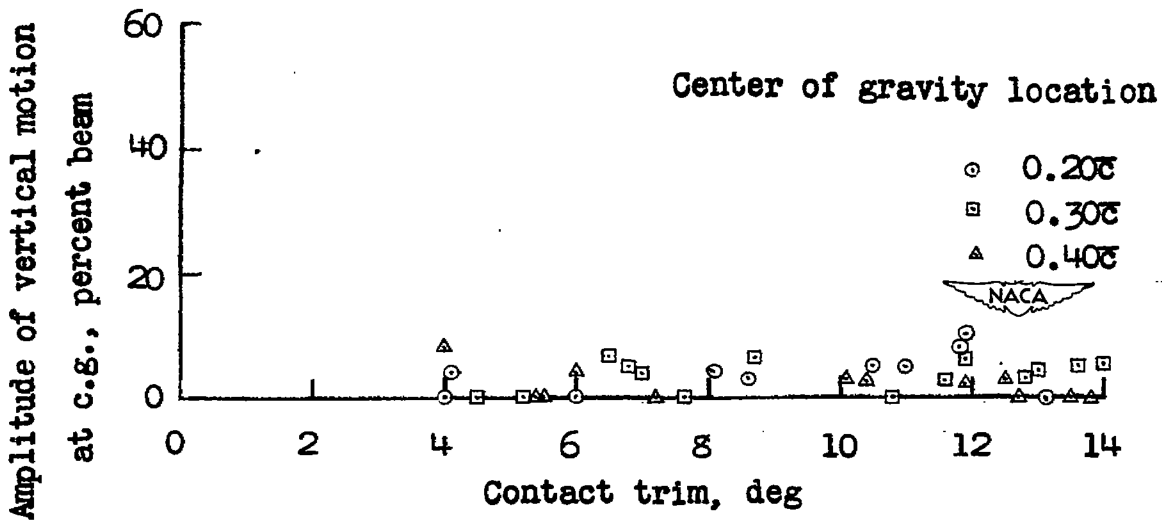

(b) Amplitudes of vertical motion.

Figure 12.– Landing stability.

[redacted]

[redacted]

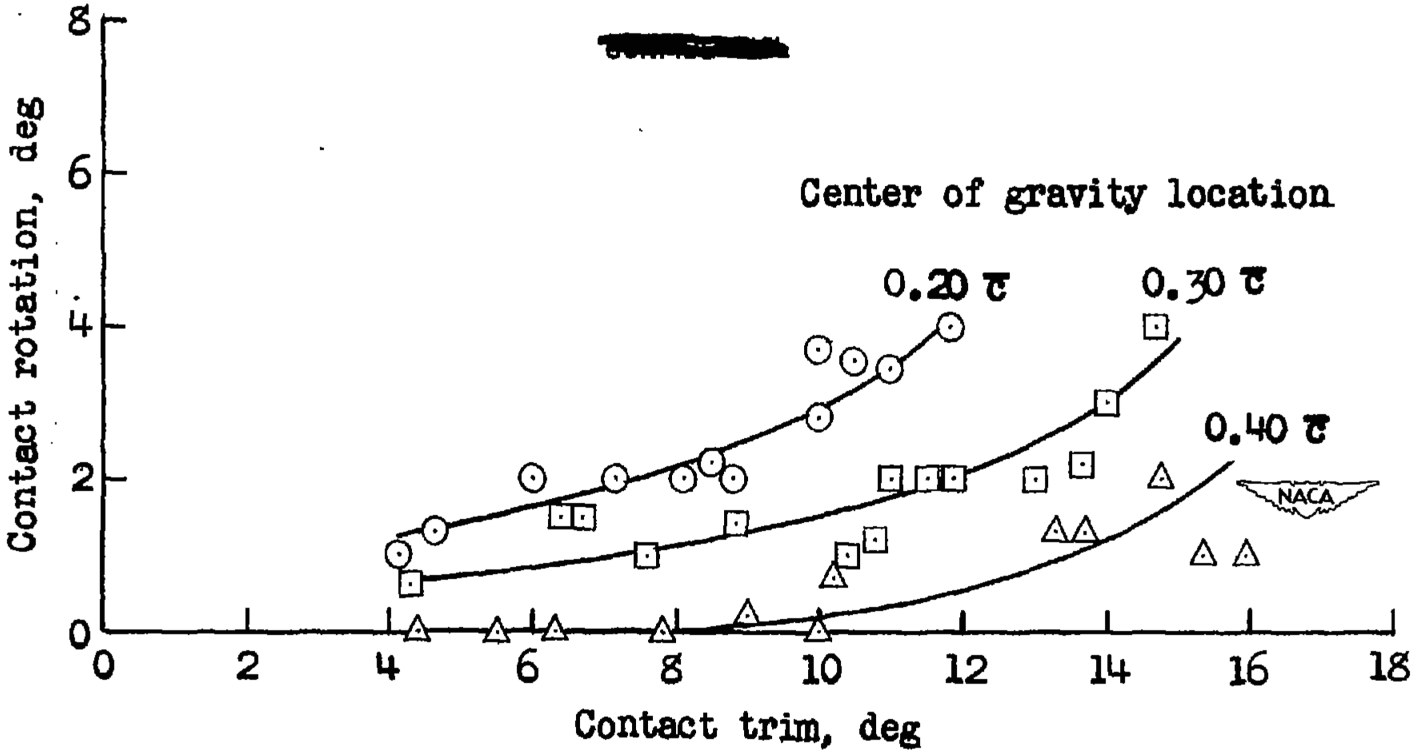

Figure 13.- Change in trim at contact.

[redacted]

[redacted]

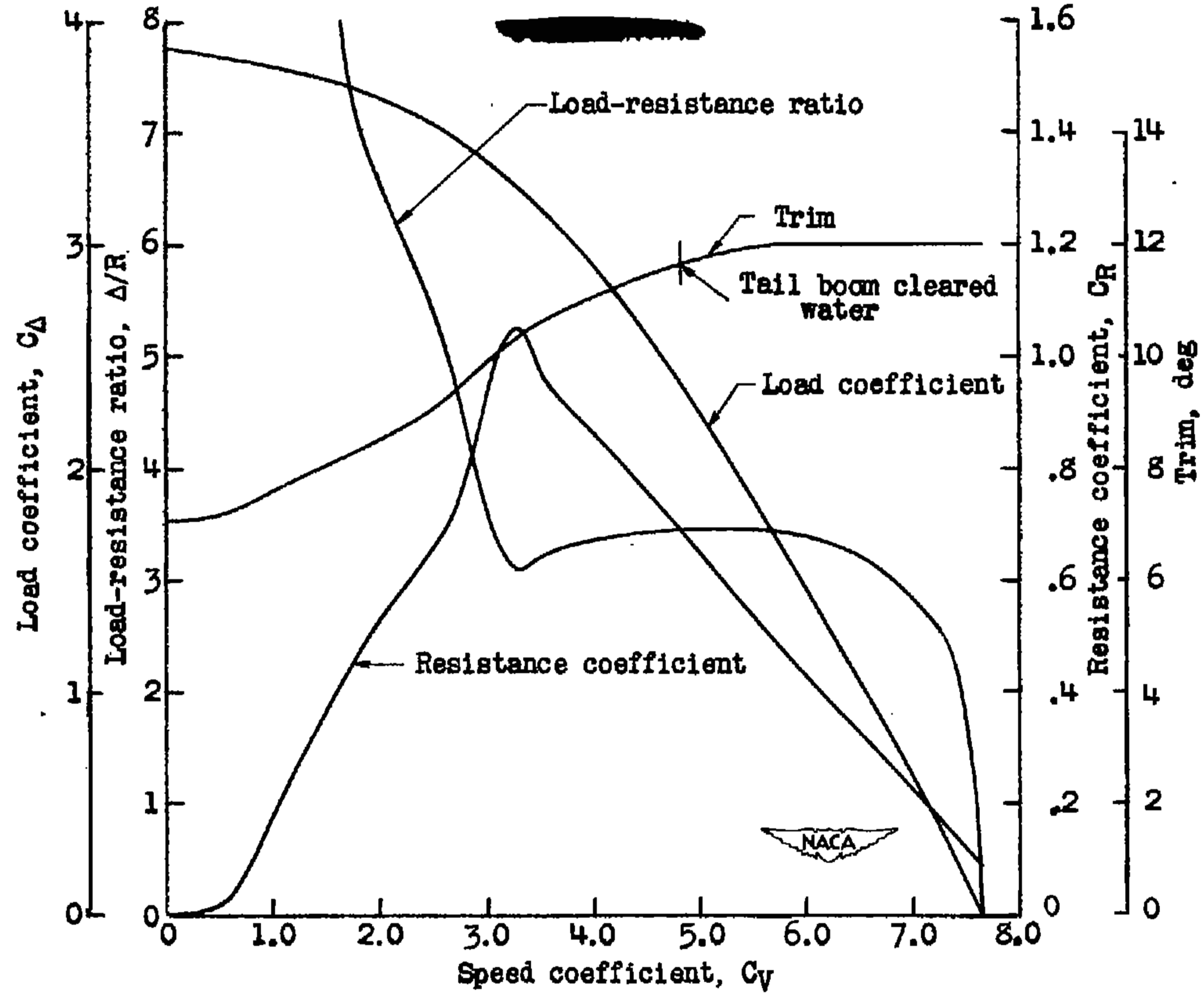

Figure 14.– Resistance coefficient, load-resistance ratio, trim and load coefficient for minimum stable resistance.

[redacted]